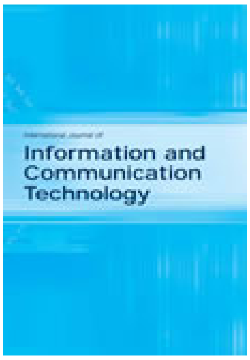

International Journal of Information and Communication Technology

ISSN online: 1741-8070 - ISSN print: 1466-6642
https://www.inderscience.com/ijict

Predicting remaining lithium-ion battery life based on multi-cycle time series models

Peide Xu, Jie Li

Article History:

Received:	24 September 2024
Last revised:	24 November 2024
Accepted:	25 November 2024
Published online:	20 January 2025

Predicting remaining lithium-ion battery life based on multi-cycle time series models

Peide Xu*

School of Power Engineering,
Fujian Polytechnic of Water Conservancy and Electric Power,
Yongan, Fujian, 366000, China
Email: 15859875552@163.com
*Corresponding author

Jie Li

School of Electric Power,
South China University of Technology,
Guangdong, Guangzhou, 510641, China
Email: 1522660260@qq.com

Abstract: We propose a novel deep learning-based model for predicting the remaining life of lithium-ion batteries. Existing methods merely model the remaining life's temporal changes, overlooking inherent time series periodicity and compromising prediction accuracy. Our model capitalises on multi-cycle features in time series analysis, using well-designed 2D temporal blocks to handle uncertainties in battery remaining useful life changes. It extracts complex patterns within charge and discharge cycles, achieving high-precision predictions of future battery states. On multiple common battery datasets, it surpasses existing methods in accuracy and robustness, validating its effectiveness.

Keywords: lithium-ion battery; remaining useful life prediction; multi-cycle time series.

Reference to this paper should be made as follows: Xu, P. and Li, J. (2025) 'Predicting remaining lithium-ion battery life based on multi-cycle time series models', *Int. J. Information and Communication Technology*, Vol. 26, No. 1, pp.55–72.

Biographical notes: Peide Xu is an Associate Professor and graduated from Sichuan Institute of Technology University in 2007. He is a Visiting Scholar of South China University of Technology and worked in Fujian Polytechnic of Water Conservancy and Electric Power. His research interests include power battery energy storage technology teaching and management.

Jie Li graduated from SCUT in 2023. He worked at TP-Link. His research interests include multi-state estimation of lithium-ion power batteries.

1 Introduction

With the development of technology, lithium-ion batteries play an irreplaceable role in various devices such as mobile communication devices (Zeng et al., 2021), electric vehicles (Smith et al., 2009), and smart devices (Serrao et al., 2011). They have been integrated into every aspect of our daily lives (Pop et al., 2007) and have profound impacts on our work and lifestyle (Raijmakers et al., 2019). However, despite the widespread application of lithium-ion batteries (Smith and Wang, 2006), accurately predicting their remaining life still poses significant challenges (Waag et al., 2014; Prusty et al., 2022c). The battery's remaining life and its intrinsic state are crucial for the normal operation of devices, prevention of unexpected shutdowns, and effective management of device lifespan. Despite significant research efforts in this area (Deng et al., 2023; Zhang, 2024), predicting the remaining life of lithium-ion batteries remains fraught with complexities due to the batteries' inherent nonlinear degradation processes and the influence of various environmental factors.

Currently, many studies (Hu et al., 2012; Sun et al., 2011; Ouyang et al., 2020; Prusty et al., 2024a) have focused on this issue and proposed various methods for predicting the remaining life of lithium-ion batteries. These methods have contributed to some extent in addressing the problem (Rahimi-Eichi et al., 2013; Kim and Cho, 2011; Prusty et al., 2022a; Patil et al., 2023), but they still have limitations and challenges. The main issue is that most existing prediction models treat the remaining life of lithium-ion batteries as a time series problem and only model the variation of capacity over time (Hu et al., 2009; Zhang et al., 2024), disregarding the inherent periodic variations within the time series (Deng et al., 2023; Eddahech et al., 2012). Traditional models primarily focus on time-domain information (Wang, 2023; Prusty et al., 2024b), neglecting the frequency changes that occur during the discharge process of lithium-ion batteries. This oversight limits the models' ability to capture the full spectrum of temporal dynamics, particularly the periodic patterns that are crucial for accurately modelling capacity degradation. This limitation hampers the accurate reflection of comprehensive changes in battery states in practical applications and subsequently affects the prediction accuracy. Furthermore, existing models (Ipek et al., 2021; Prusty et al., 2022b) often assume a fixed charging and discharging cycle for batteries, failing to account for the variations in frequency and other periodic characteristics that can significantly impact the battery's performance over time. A more holistic approach, which incorporates both time-domain and frequency-domain features, is essential for enhancing the precision of remaining life predictions. Besides, factors such as temperature, load, and aging can impact the charging and discharging cycles, leading to variations in battery capacity (Farmann et al., 2015; Li et al., 2023). As a result, existing models fail to accurately predict the dynamic changes in battery remaining life (He et al., 2011b; Chen et al., 2022; Li et al., 2020).

Our key contribution is a novel multi-cycle time series model for battery remaining life prediction. We integrate time- and frequency-domain features, enabling comprehensive analysis of periodic and complex patterns in charge-discharge cycles. Below, we summarise the key contributions:

- Multi-cycle modelling framework: unlike traditional methods (e.g., LSTM, CNN) that predominantly rely on time-series capacity trends, our approach models the inherent periodic patterns in charge-discharge cycles by combining time- and frequency-domain features. This holistic modelling improves the understanding of complex battery degradation dynamics.

- 2D time block innovation: by introducing 2D time blocks, our model effectively captures hidden temporal and spatial correlations within charge-discharge cycles, adapting to uncertainties in battery states and environmental variations.
- Enhanced robustness and accuracy: our approach outperforms state-of-the-art deep learning models by capturing both transient and long-term variations in battery behaviour, ensuring higher accuracy and robustness across diverse environmental and aging conditions.
- Practical applicability: the model's ability to adapt to varying operational conditions and its interpretability make it highly practical for real-world applications, setting a new benchmark for battery life prediction techniques.

2 Materials and methods

2.1 Data collection and preprocessing

In the experiment, we utilised the CALCE dataset from the University of Maryland, USA (Xing et al., 2013). To enhance the diversity and reliability of our experiment, we selected data from CS2 batteries under two distinct constant current conditions. Specifically, we employed the CS2_33 and CS2_34 dataset cycled at a constant current condition of 0.5C, along with the CS2_35, CS2_36, CS2_37, and CS2_38 datasets cycled at a constant current condition of 1C.

During the experiment, all CS2 batteries followed an identical charging protocol. The charging process adopted the standard constant current/constant voltage (CC/CV) scheme, applying a steady current until the voltage reached 4.2 V, after which the voltage was sustained at 4.2 V until the charging current fell below 0.05 A. Additionally, the cut-off voltage for discharging these CS2 batteries was set to 2.7 V, considered as the critical voltage indicating the end of discharge. The charging process and cut-off voltage were meticulously set to ensure the consistency and comparability of the experiment, guaranteeing that all CS2 batteries underwent the same protocol during testing. The strategy facilitates a more effective comparison and analysis of battery performance and characteristics.

Following this experimental setup, we defined the inputs and outputs for our predictive model. The model input is a time series representing the historical data of battery capacity, denoted as $X = \{x_1, x_2, \ldots, x_t\}$, where x_t indicates the observed capacity at time step t. The output of the model is the predicted remaining capacity at a future time step, represented as $\hat{y}_{t+k}$, where k is the prediction horizon. The overall goal is to minimise the difference between the predicted capacity $\hat{y}_{t+k}$ and the true capacity y_{t+k} over the prediction period.

The prediction problem is formulated as a supervised learning task, where the model is trained to learn the mapping function $f : X \rightarrow \hat{y}_{t+k}$ that best approximates the relationship between historical capacity data and future capacity. The loss function

$L(y_{t+k}, \hat{y}_{t+k})$, typically mean squared error (MSE), is used to quantify the prediction error, and the model is optimised to minimise this loss over the training dataset.

2.2 Multi-cycle time series model design

To address the limitations of existing prediction methods in capturing the periodic variations in the time series of lithium-ion battery remaining life, we propose a novel multi-cycle time series model. The model aims to achieve high precision prediction of remaining life by effectively extracting and learning complex patterns within the battery charging and discharging cycles. Figure 1 details the main components and design principles of the model.

2.3 Normalisation and embedding

Considering the disparate scales among different datasets, which can impede model training and convergence, it is essential to normalise the data. Normalisation allows for a more accurate representation of the battery's remaining life at different time points and mitigates the influence of scale differences on the prediction outcomes. Specifically, if we denote the original data as X with a mean of μ and a standard deviation of σ, the data can be normalised using the following formula:

$$X_{normalised} = (X - \mu)/\sigma \tag{1}$$

Here, X represents the dataset values, which include variables such as battery capacity, voltage, or current at different time points. Normalising these variables standardises their scale, thus facilitating more effective model training. In the preliminary stage of data representation, we utilised two embedding approaches: token embedding and position embedding. These embedding techniques are instrumental in converting the data into a format suitable for model processing while enhancing the representation of features. To begin, we transformed each remaining life value $x(t)$, for every time step t, into a high-dimensional vector using token embedding.

The conversion was accomplished by applying one-dimensional convolution, as depicted by the following formula:

$$T(t) = f(W * x(t) + b) \tag{2}$$

where W represents the weights of the convolutional kernel, b denotes the bias term, $*$ denotes the convolution operation, and f refers to an activation function (such as ReLU). The objective of token embedding is to capture and represent the semantic information of each token. In this context, tokens refer to the battery's state at specific time steps. Through one-dimensional convolution, the model can capture the local information of each token and identify the relationships among these local features.

Subsequently, we introduce position embedding to incorporate the positional information of elements within the sequence. Position embedding employs the position encoding method derived from the transformer model. By adding position encoding vectors to the token embedding vectors, we represent the positional characteristics of the elements. For each position i, the position encoding vector PE is calculated using the following formula:

$$PE_{(pos,2i)} = \sin\left(pos/10{,}000^{2i/d_{model}}\right) \tag{3}$$

$$PE_{(pos,2i+1)} = \cos\left(pos/10{,}000^{2i/d_{model}}\right) \tag{4}$$

where i represents the dimension of the position encoding vector. pos denotes the position of the element in the sequence. Note that we utilise a hyperparameter d_{model} to control the dimensionality of the position encoding vector. Subsequently, we add the position encoding vector to the token embedding vector, resulting in the final position embedding $E_{position}$ with the following formula:

$$E_{position} = T_{token} + PE_{pos} \tag{5}$$

By employing token embedding and position embedding, we transform the original data into vector representations that possess meaningful characteristics. The representation effectively retains the local features and temporal relationships within the data, thereby facilitating subsequent model training and prediction tasks.

Figure 1 The overall flow of our architecture, (a) data preprocessing module, where raw battery data is cleaned and filtered to remove noise and outliers, ensuring the quality of the input data, (b) data normalisation and embedding module, in which the preprocessed data is normalised to a consistent scale and then embedded into a suitable feature space for model input, (c) time series feature encoding module, where the temporal characteristics of the data are captured and encoded, allowing the model to learn complex patterns over time, (d) the specific training process of the model, detailing how the model extracts 2D temporal features from 1D time series data (see online version for colours)

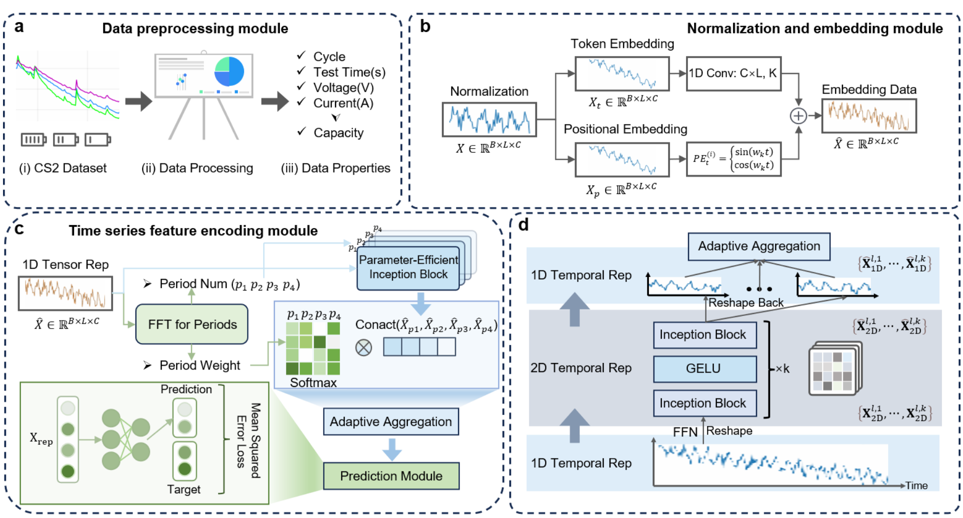

2.4 Denoising and periodic patterns

The data representing the remaining life of lithium-ion batteries often contains noise, which may stem from measurement errors, variations in usage patterns, or the influence of environmental factors, among others. The noise can affect the clarity of the data and subsequently impact the accuracy of battery performance analysis and prediction on the other hand, battery usage patterns may exhibit certain periodic patterns. For instance, users may charge their batteries at specific times of the day, or certain devices may undergo regular charging and discharging operations at fixed intervals. These periodic patterns are valuable for understanding battery usage patterns and predicting remaining life.

The introduction of 2D temporal blocks enables the representation of temporal correlations and periodic patterns in a two-dimensional grid, similar to how convolutional layers in CNNs capture spatial features in images (Bai et al., 2018). Studies such as (Durairaj and Mohan, 2022) have demonstrated the benefits of converting time-series data into 2D representations to enhance pattern recognition, particularly in applications involving periodicity or multiscale dependencies.

Fast Fourier transform (FFT) (Pfister, 2017) has been widely used to extract frequency-domain features from time-series data, providing insights into hidden periodic patterns that are often overlooked by purely time-domain models. Previous works, such as those by He et al. (2011a) and Zhao and Liu (2025), have validated the effectiveness of combining frequency-domain analysis with deep learning to improve prediction accuracy in systems with nonlinear and periodic behaviours. Additionally, working in the frequency domain facilitates noise reduction techniques. For instance, smoothing the data by eliminating high frequency components (typically associated with noise) using filters can effectively minimise the impact of noise.

More specifically, let represent the preprocessed time series data as $E(t)$, where $t = 1, 2, \ldots, N$, and N denotes the total number of data points in the sequence. The time series $E(t)$ consist of measurements such as the battery's voltage, current, or capacity over time. To capture the frequency components of this time series data, which reflect periodic patterns within the battery's performance, we employ the fast Fourier transform (FFT). The FFT is used to convert the time-domain data into the frequency domain, as shown in the following formula:

$$F(k) = \frac{1}{N}\sum\nolimits_{t=1}^{N} E(t)e^{-i2\pi kt/N} \tag{6}$$

where $F(f)$ represents the data in the frequency domain, with $k = 0, 1, \ldots, N - 1$. The exponential term $e^{-i2\pi kt/N}$ serves as the basis function for each frequency component. The transformation to the frequency domain allows us to decompose the time series into its constituent frequency components, each characterised by an amplitude $A(k)$ and phase $\phi(k)$ calculated as:

$$A(k) = |F(k)| \tag{7}$$

$$\phi(k) = \arg(F(k)) \tag{8}$$

In the context of battery capacity prediction, not all frequencies are equally important. High-frequency components may represent noise rather than meaningful periodic behaviour. Therefore, we focus on the most significant frequencies, which correspond to the largest amplitudes. Let these significant frequencies be denoted as $f_1, f_2, \ldots, f_k$. The corresponding period lengths $T_1, T_2, \ldots, T_k$ are derived from these frequencies, where $T_i = 1/f_i$. Each period T_i represents a distinct cycle within the battery's operation, such as charging, discharging, or resting phases. By identifying these cycles, we can reshape the one-dimensional time series $E(t)$ into multiple two-dimensional tensors. Each tensor reflects the variations in the time series under a specific period, allowing the model to analyse the data in a way that aligns with the natural cycles of the battery's operation.

$$\mathbf{E}_{2D}^{i} = \text{Reshape}_{T_i, f_i}\left(\text{Padding}\left(\mathbf{E}_{1D}\right)\right), \qquad i \in \{1, \ldots, k\} \tag{9}$$

where $\text{Reshape}_{T_i, f_i}$ denotes the dimensional transformation of the original time series data based on the period length and frequency, and Padding represents padding the time series data.

The approach enhances the model's ability to predict the battery's remaining life by leveraging both time-domain and frequency-domain information. It captures complex patterns and periodicities that are critical for accurately forecasting future battery performance.

2.5 Inception module and adaptive aggregation

In our task of predicting the remaining battery life, we have adapted the design of the inception module to process multiple two-dimensional tensors derived from the FFT (Szegedy et al., 2015). The FFT converts the time-series data of battery parameters, such as voltage, current, and capacity, into the frequency domain, enabling us to capture essential periodicities in the battery's operational patterns. The inception module is particularly suited for this task as it allows us to capture data characteristics across different scales by utilising multiple convolutional kernels of varying sizes in parallel. The multi-scale processing is crucial for effectively analysing the complex and varied frequency components inherent in the battery data.

In our approach, we input each two-dimensional tensor, derived from the FFT, into an independent inception module. The inception module is composed of multiple convolutional layers designed to extract features at various scales. Specifically, we utilise 2D convolution modules with different sized convolution kernels to capture information at differing scales. The outputs from these modules are then aggregated, resulting in a new feature representation.

$$\mathbf{E}_{2D}^{l,i} = \text{Inception}\left(\mathbf{E}_{2D}^{l,i}\right), \qquad i \in \{1, \ldots, k\} \tag{10}$$

$$\hat{\mathbf{E}}_{2D}^{all} = Concat\left(\hat{\mathbf{E}}_{2D}^{l,i}\right), \qquad l \in \{1, \ldots, n\} \tag{11}$$

where l denotes the number of layers in the inception module, while i refers to the i^{th} frequency component. Thus, for each layer of the inception module, we obtain a corresponding feature representation $\hat{\mathbf{E}}_{2D}^{l,i}$. The represents the output of the i^{th} two-dimensional tensor under the l^{th} inception block, post-inception module processing. Subsequently, we aggregate the feature representations $\hat{\mathbf{E}}_{2D}^{l,i}$ across all periods, forming a comprehensive new feature representation $\hat{\mathbf{E}}_{2D}^{all}$. The aggregation process ensures that features extracted from all relevant scales are integrated, enhancing the model's ability to capture multi-scale temporal variations in the battery's remaining charge.

To further refine the feature representation, we apply an adaptive aggregation strategy. The significance of each feature representation across different periods is evaluated by calculating the amplitude A_i for each feature representation $\hat{\mathbf{E}}_{1D}^{i}$ under each period:

$$A_i = \left|\hat{\mathbf{E}}_{1D}^{i}\right|, \qquad i \in \{1, \ldots, k\} \tag{12}$$

Next, we carry out softmax normalisation on the amplitude values, resulting in aggregation weights represented by w:

$$w_i = \operatorname{softmax}\left(A_1, \ldots, A_k\right) \tag{13}$$

Finally, by multiplying each feature representation $\hat{\mathbf{E}}_{1D}^{i}$ by its corresponding aggregation weight w, and summing them up, we integrate these feature representations to form the ultimate aggregated result $\mathbf{E}_{1D}^{l}$.

$$\mathbf{E}_{1D}^{l} = \sum_{i=1}^{k} w_i \times \mathbf{E}_{2D}^{l,i} \tag{14}$$

The adaptive aggregation process allows the model to prioritise the most significant frequency components, which are most indicative of the battery's remaining life, thereby creating a robust global feature representation. By integrating the inception module with adaptive aggregation, our approach effectively captures and processes multi-scale temporal variations in the battery data, leading to improved prediction accuracy. Our method leverages both the time-domain and frequency-domain characteristics of the battery's operational data, making it a powerful tool for modelling and predicting the remaining life of lithium-ion batteries.

3 Experiments

3.1 Baselines

Our method uniquely aims at predicting future capacity changes based on historical capacity data, which is a novel perspective not extensively explored in prior work. To evaluate the effectiveness of our novel approach, we conducted a comparative analysis with three widely recognised models: long short-term memory (LSTM) (Graves and Graves, 2012), gated recurrent unit (GRU) (Cho et al., 2014), and convolutional neural network (CNN) (Kim and Kim, 2017). These models serve as baselines in our study, providing a benchmark against which the performance of our method can be assessed. The comparative analysis aims to empirically validate the superiority of our approach in modelling and predicting the remaining battery capacity. Detailed discussion and analysis of these comparisons are presented in the subsequent sections, further substantiating the advantages of our methodology.

3.2 Evaluation metrics

We employ three key metrics to evaluate the performance of our proposed model: the relative error (RE), mean absolute error (MAE), root mean square error (RMSE) and R^2 score. The RE is defined as the ratio of the difference between the actual and predicted cycle counts when the battery capacity degrades to the failure threshold to the actual value. The MAE and RMSE refer to the average absolute error and root mean square error, respectively, between the predicted and actual capacity values. The coefficient of determination (R^2) measures the proportion of the variance in the dependent variable that is predictable from the independent variables. An R^2 score closer to 1 indicates that the model explains most of the variance in the remaining battery capacity, providing an overall measure of the model's goodness-of-fit. The formulas for their calculation are as follows:

$$RE = \frac{C - \hat{C}}{C} \tag{15}$$

$$MAE = \frac{1}{n} \sum_{i=1}^{n} \left| y_i - \hat{y}_i \right| \tag{16}$$

$$RMSE = \sqrt{\frac{1}{n} \sum_{i=1}^{n} \left(y_i - \hat{y}_i \right)^2} \tag{17}$$

$$R^2 = 1 - \frac{\sum_{i=1}^{n} \left(y_i - \hat{y}_i \right)^2}{\sum_{i=1}^{n} \left(y_i - \overline{y} \right)^2} \tag{18}$$

where n represents the total number of cycles, y_i and $\hat{y}_i$ denote the actual and predicted remaining battery capacity at the i^{th} cycle, respectively. Additionally, C and $\hat{C}$ correspond to the actual and predicted number of cycles when the capacity degrades to the failure threshold. These three metrics together allow for a well-rounded evaluation of our model's accuracy, robustness, and reliability in predicting the remaining battery charge.

3.3 Experiment setup

In this study, we employed a combination of time-domain and frequency-domain features in our model to predict the remaining capacity of lithium-ion batteries. The model was configured using standard hyperparameters commonly used in deep learning tasks. The training process was optimised using the Adam optimiser with a learning rate of 0.001. The model was trained over 200 epochs with a batch size of 32, with early stopping to prevent overfitting when the validation loss plateaued.

To evaluate the generalisation of the model, we applied 5-fold cross-validation, ensuring the model was trained on multiple data splits and tested on each to provide a robust estimate of its performance. The method allows for a more accurate assessment by reducing the bias of a single training-test split.

To ensure the optimal performance of our model, we employed a grid search to systematically explore various combinations of key hyperparameters, including learning rate, batch size, number of hidden units, and dropout rate. Specifically, we tested learning rates in the range of 0.0001, 0.001, and 0.01, batch sizes of 16, 32, and 64, and hidden unit configurations of 64, 128, and 256 units. Additionally, we evaluated dropout rates of 0.2, 0.3, and 0.5 to mitigate overfitting. The optimal hyperparameters were selected based on the lowest validation loss, using 5-fold cross-validation and mean squared error (MSE) as the performance metric.

3.4 Performance of the proposed methods

Our experiment adopted a unique data partition strategy that aligns more accurately with real-world battery usage. Specifically, we employed the first 50% of the data for training and the latter 50% for testing. This data splitting methodology is based on the rationale that in real-world scenarios, battery usage does not occur randomly; instead, the early usage data (train set) is used to predict the subsequent usage (test set). By applying this sequential data split, our model's learning process better mimics the progressive nature of battery degradation. It enables the model to be trained on the initial degradation patterns and then to validate its predictive capabilities on the later degradation behaviours.

Table 1 Predicted results of constant current discharge at 0.5C

Battery	*Metric*	*LSTM*	*GRU*	*CNN*	*Ours*
CS2_33	RE	0.241	0.241	0.158	0.021
	MAE	0.082	0.081	0.063	0.013
	RMSE	0.096	0.094	0.088	0.020
	R^2	0.812	0.810	0.914	0.998
CS2_34	RE	0.241	0.253	0.102	0.020
	MAE	0.052	0.054	0.023	0.011
	RMSE	0.059	0.061	0.032	0.019
	R^2	0.876	0.871	0.956	0.998

Figure 2 Predicted results of constant current discharge at 0.5C (see online version for colours)

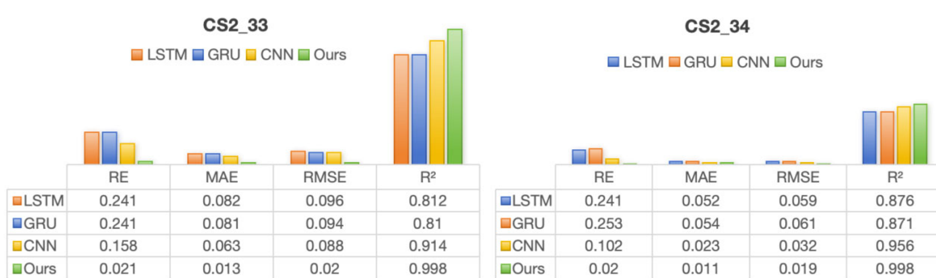

The experimental results, as shown in Tables 1 and 2, provide compelling evidence of the superior performance of our proposed method compared to the conventional models (LSTM, GRU, CNN) under both 0.5C and 1C constant current discharge conditions. Under 0.5C discharge condition, our model consistently outperforms the other models. For instance, considering battery CS2_33, our model achieves the relative error (RE) of 0.021, mean absolute error (MAE) of 0.013, and root mean square error (RMSE) of 0.020. These are significantly lower than the corresponding values for LSTM (RE: 0.241, MAE: 0.082, RMSE: 0.096), GRU (RE: 0.241, MAE: 0.081, RMSE: 0.094), and CNN (RE: 0.158, MAE: 0.063, RMSE: 0.088). Similar trends can be seen with battery CS2_34.

Table 2 Predicted results of constant current discharge at 1C

Battery	*Metric*	*LSTM*	*GRU*	*CNN*	*Ours*
CS2_35	RE	0.267	0.273	0.207	0.035
	MAE	0.058	0.058	0.046	0.015
	RMSE	0.071	0.071	0.064	0.025
	R^2	0.805	0.800	0.890	0.990
CS2_36	RE	0.392	0.409	0.170	0.034
	MAE	0.063	0.061	0.050	0.014
	RMSE	0.072	0.069	0.064	0.019
	R^2	0.755	0.745	0.916	0.996
CS2_37	RE	0.301	0.305	0.174	0.004
	MAE	0.055	0.054	0.039	0.010
	RMSE	0.065	0.064	0.054	0.014
	R^2	0.803	0.795	0.906	0.999
CS2_38	RE	0.139	0.140	0.108	0.023
	MAE	0.051	0.051	0.037	0.012
	RMSE	0.062	0.061	0.050	0.019
	R^2	0.888	0.880	0.936	0.997

Figure 3 Predicted results of constant current discharge at 1C (see online version for colours)

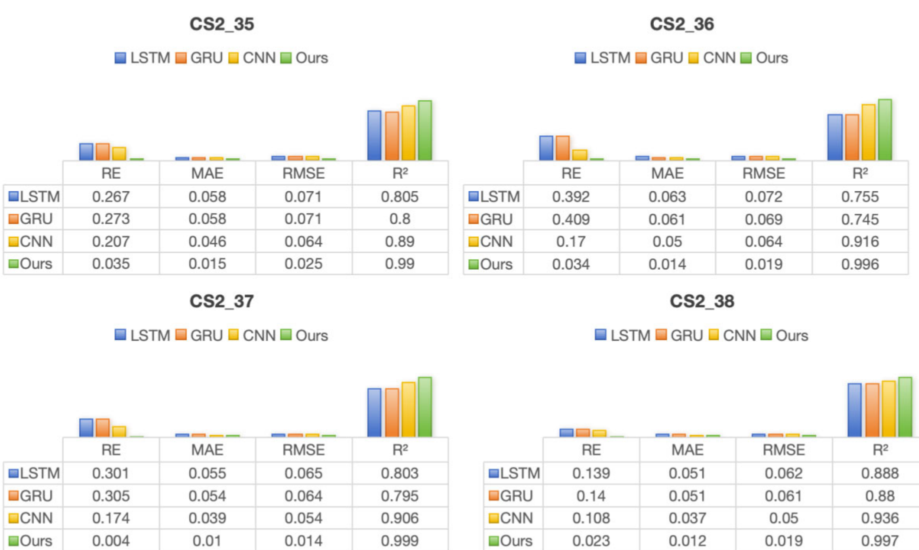

Table 2 reveals the same superior performance of our proposed method when the discharge current was increased to 1C. For all tested batteries (CS2_35, CS2_36, CS2_37, and CS2_38), our model consistently produced lower RE, MAE, and RMSE than the baselines. It is notable that our model achieved an exceptionally low RE of 0.004 for the battery CS2_37, which far outstrips the performance of the other methods.

Figure 4 Predicted capacity of constant current discharge at 0.5C, (a) CS2_33 dataset (b) CS2_34 dataset (see online version for colours)

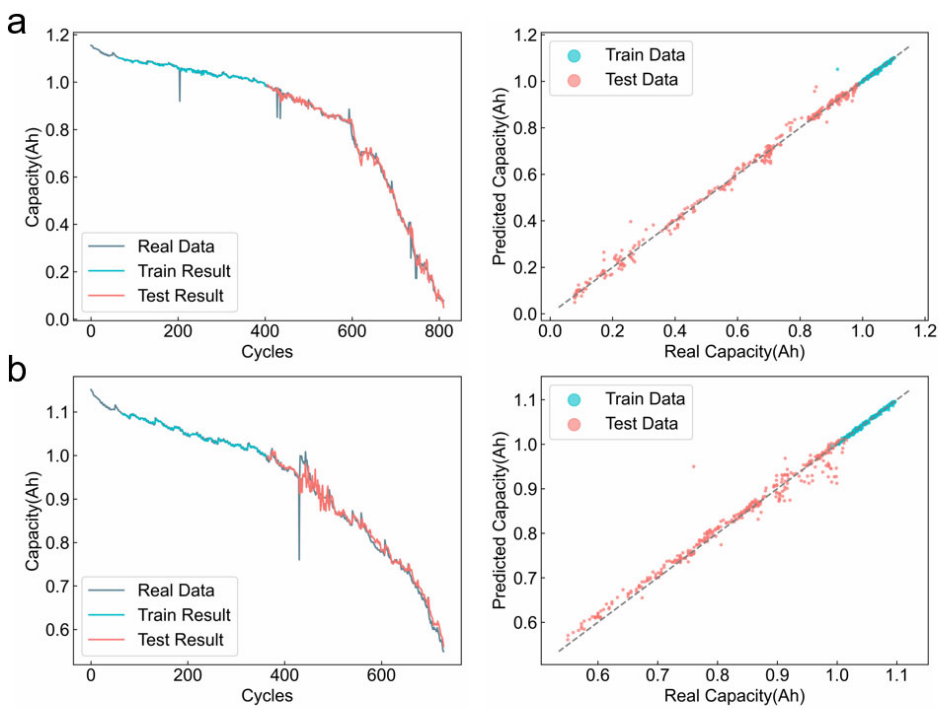

The remarkable results from our proposed method under both discharge conditions signify that our model exhibits superior prediction accuracy, robustness, and reliability in predicting the remaining battery charge. The advantage of our model becomes particularly pronounced when we consider the critical role of battery lifespan prediction in practical scenarios such as electric vehicles and portable electronics, where accurate and reliable predictions can lead to improved energy management, efficiency, and longevity of these devices.

3.5 Representation analysis

In this section, we interpret the performance of our model from the standpoint of representation learning. As suggested by Figures 4 and 5, our model exhibits an excellent fit to the actual data in both training and testing stages, underscoring its potent learning and generalisation capabilities in this complex task.

Firstly, for the training phase, the high concordance between the model's predictions and the actual data unveils the model's deep understanding of the intrinsic patterns in the data and the physical processes of battery discharging behaviour. This is vital for designing efficient battery management systems (BMS), as a model that comprehends the dynamic behaviours of the battery can predict the remaining battery life more accurately. Secondly, in the testing phase, despite being exposed to unseen data, the model still yields accurate predictions of the remaining battery life, indicating its robust generalisation capabilities. This suggests that our model not only learns and comprehends the behavioural patterns of the battery from the training data but also retains its predictive precision in unseen data, demonstrating its strong robustness.

For all batteries, the prediction results under different discharge currents demonstrate that our model excels in all evaluation metrics (including RE, MAE, and RMSE), outperforming LSTM, GRU, and CNN, whether under a discharge current of 0.5C or 1C. This further substantiates the superiority and comprehensiveness of our model in handling the task of predicting the remaining battery life. In summary, these results strongly suggest that our model exhibits outstanding performance, robust generalisation capabilities, and robustness in the task of predicting the remaining battery life of batteries.

3.6 Long-term predictive performance analysis

In this experiment, we have designed a new prediction approach. Similarly to the previous setting, we constructed data with a length of 32 time points as the model's observations.

However, our prediction length is not 1, but a longer time dimension, which has never been seen in current papers on lithium-ion battery remaining life prediction. The experimental results are shown in Table 3. Despite the sharp increase in prediction difficulty, our model is able to maintain high performance for predicting battery charge values with two different charging rates. Compared to the MAE and RMSE of the prediction length of 1, the model does not show any performance degradation, indicating that our model has good robustness. In contrast, traditional deep learning models experience a significant decline in performance when facing long-term prediction due to the increase in task difficulty. The specific explanation is as follows:

1 by using token encoding and position encoding, our model can preserve more effective information when converting the original charge data to the latent space

2 by using FFT to convert time domain signals to the frequency domain, we can better analyse the frequency spectrum characteristics of the signals and perform signal filtering, which is important for removing noise and extracting key signal features from lithium-ion battery data

3 through efficient inception modules and adaptive aggregation, our model can not only capture 1D information but also capture potential pattern information ignored by existing methods at higher dimensions.

This is why our model can maintain good performance even when facing long-term prediction.

To visually reveal the prediction process of the model, we conducted a visual analysis using a single task from the test set of each dataset. The results are presented in Figures 6. Through observation of these charts, it can be seen that:

1 The model we proposed is able to closely surround the label value during the prediction process, demonstrating high prediction accuracy. This indicates that our proposed model has good generalisation performance when dealing with different datasets and tasks.

2 In contrast, the prediction results of traditional deep learning models have a large error range around the label value, suggesting that the performance of traditional models in similar tasks may be influenced by factors such as dataset distribution and model architecture.

3 By comparing and analysing the results, we can see that the model we proposed performs more consistently and reliably with higher prediction accuracy.

It provides valuable reference for solving related problems. To achieve better prediction results, future research can further explore optimisation strategies for the model, such as improving network architecture and optimising learning algorithms. In addition, the model can be transferred and adjusted to adapt to different application scenarios in different fields. Through in-depth research and practice, we believe that the model we proposed will play a more important role in related fields and provide more accurate and reliable prediction support for solving practical problems.

Table 3 Long-term predictive result for two distinct constant current discharge rates

Battery	*CS2_33*		*CS2_34*		*CS2_35*	
Metric	*MAE*	*RMSE*	*MAE*	*RMSE*	*MAE*	*RMSE*
LSTM	0.128	0.154	0.104	0.123	0.108	0.131
GRU	0.122	0.149	0.088	0.101	0.100	0.121
CNN	0.075	0.109	0.044	0.061	0.056	0.080
Ours	0.015	0.022	0.014	0.014	0.015	0.025
Battery	*CS2_36*		*CS2_37*		*CS2_38*	
Metric	*MAE*	*RMSE*	*MAE*	*RMSE*	*MAE*	*RMSE*
LSTM	0.114	0.138	0.107	0.128	0.104	0.125
GRU	0.106	0.129	0.098	0.118	0.097	0.116
CNN	0.065	0.093	0.049	0.071	0.050	0.074
Ours	0.017	0.022	0.014	0.020	0.015	0.022

Figure 5 Predicted capacity of constant current discharge at 1C, (a) CS2_35 dataset (b) CS2_36 dataset (c) CS2_37 dataset (d) CS2_38 dataset (see online version for colours)

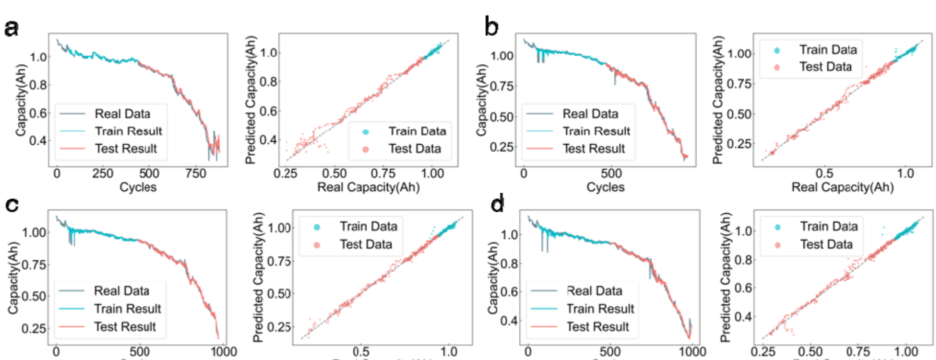

Note: In each subfigure, the left chart shows the trend of remaining life over cycles, while the right chart represents the relationship between the predicted remaining life and the actual capacity.

Figure 6 Long-term predictions are conducted under constant current discharges of 0.5C and 1C, for 0.5C, (a) CS2_33 (b) CS2_34; for 1C, (c) CS2_35 (d) CS2_36 (e) CS2_37 (f) CS2_38 (see online version for colours)

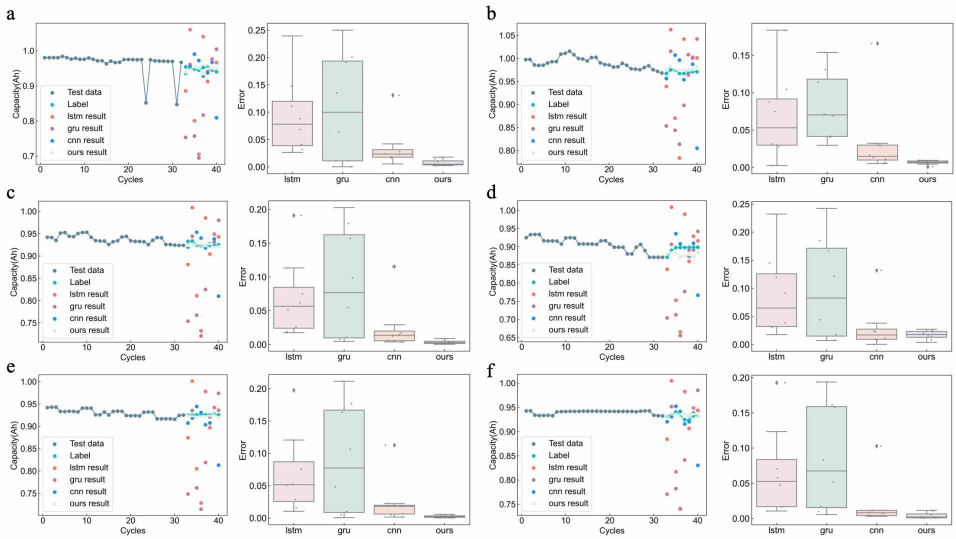

Note: In each dataset, the left figure illustrates the prediction results of different models, while the right figure presents the errors of the prediction results. The test data represents the actual capacity changes of the lithium-ion battery, while the label still refers to the remaining life measured through experiments. The term 'label' is used here to differentiate it from the portion used for training.

4 Discussion

4.1 Limitations of using a single dataset

The current model is trained and validated on a dataset derived from a specific type of lithium-ion battery under controlled conditions. This focus may limit its applicability to other battery chemistries, such as lithium iron phosphate ($LiFePO_4$) or nickel-manganese-cobalt (NMC) batteries, which exhibit different degradation characteristics and charging/discharging behaviours.

A single dataset often captures battery behaviour under specific environmental factors, such as temperature and load, which may not represent the full range of real-world operating conditions. This could reduce the model's robustness when applied to batteries operating in diverse or extreme conditions.

The dataset may have inherent biases, such as covering only a limited portion of the battery's lifecycle, which can result in suboptimal performance for predicting end-of-life behaviours or anomalies.

4.2 Proposed extensions to other battery types

Expanding the model's validation to datasets from different battery chemistries and manufacturers would allow for a comprehensive evaluation of its generalisability.

Publicly available datasets, such as the CALCE dataset or those from NASA's Prognostics Center of Excellence, could be leveraged for this purpose.

For better adaptability, features specific to different battery chemistries (e.g., impedance characteristics, state of health parameters) could be integrated into the model. Using datasets that combine laboratory measurements with real-world operational data can help improve robustness and applicability to diverse scenarios.

5 Conclusions

In this paper, we addressed the limitations of traditional lithium-ion battery remaining life prediction methods by introducing a novel deep learning model. By leveraging multi-cycle features of time series and utilising 2D temporal blocks, our model efficiently adapts to changes in battery states and provides high precision predictions. On testing with several common battery datasets, our model showed significant improvements over existing prediction methods, validating its effectiveness in terms of both accuracy and robustness. Notably, the model demonstrated its ability to maintain high predictive performance when environmental conditions changed or batteries underwent different degrees of aging.

In conclusion, the introduction of our model signifies a crucial advancement in lithium-ion battery technology. It offers a more accurate way of predicting the remaining battery charge, thereby enhancing the overall performance and lifespan of these batteries. For future work, we plan to continue refining our model by incorporating more complex real-world factors and applying it to a broader range of lithium-ion batteries.

Acknowledgements

This work was supported by Guangdong Province Key Field R&D Plan Project (No. 2021B0101230003).

References

Bai, S. et al. (2018) *An Empirical Evaluation of Generic Convolutional and Recurrent Networks for Sequence Modeling*, arXiv preprint arXiv:1803.01271.

Chen, D., Hong, W. and Zhou, X. (2022) 'Transformer network for remaining useful life prediction of lithium-ion batteries', *IEEE Access*, Vol. 10, pp.19621–19628, DOI: 10.1109/ACCESS. 2022.3151975.

Cho, K. (2014) *Learning Phrase Representations Using RNN Encoder-Decoder for Statistical Machine Translation*, arxiv preprint arxiv:1406.1078.

Cho, K., Van Merriënboer, B., Gulcehre, C. et al. (2014) *Learning Phrase Representations Using RNN Encoder-Decoder for Statistical Machine Translation*, arXiv preprint arXiv:1406.1078.

Deng, Z., Xu, L., Liu, H., Hu, X., Duan, Z. and Xu, Y. (2023) 'Prognostics of battery capacity based on charging data and data-driven methods for on-road vehicles', *Applied Energy*, Vol. 339, p.120954, ISSN 0306-2619, https://doi.org/10.1016/j.apenergy.2023.120954 [online] (https://www.sciencedirect.com/science/article/pii/S0306261923003185.

Durairaj, D.M. and Mohan, B.K. (2022) 'A convolutional neural network based approach to financial time series prediction', *Neural Computing and Applications*, Vol. 34, No. 16, pp.13319–13337.

Eddahech, A., Briat, O., Bertrand, N. et al. (2012) 'Behavior and state-of-health monitoring of Li-ion batteries using impedance spectroscopy and recurrent neural networks', *International Journal of Electrical Power & Energy Systems*, Vol. 42, No. 1, pp.487–494.

Farmann, A., Waag, W., Marongiu, A. et al. (2015) 'Critical review of on-board capacity estimation techniques for lithium-ion batteries in electric and hybrid electric vehicles', *Journal of Power Sources*, Vol. 281, pp.114–130.

Graves, A. and Graves, A. (2012) 'Long short-term memory', *Supervised Sequence Labelling with Recurrent Neural Networks*, pp.37–45.

He, H. et al. (2011a) 'State-of-charge estimation of the lithium-ion battery using an adaptive extended Kalman filter based on an improved Thevenin model', *IEEE Transactions on Vehicular Technology*, Vol. 60, No. 4, pp.1461–1469.

He, W., Williard, N., Osterman, M. et al. (2011b) 'Prognostics of lithium-ion batteries based on Dempster-Shafer theory and the Bayesian Monte Carlo method', *Journal of Power Sources*, Vol. 196, No. 23, pp.10314–10321.

Hu, X., Li, S. and Peng, H. (2012) 'A comparative study of equivalent circuit models for Li-ion batteries', *Journal of Power Sources*, Vol. 198, pp.359–367.

Hu, Y., Yurkovich, S., Guezennec, Y. et al. (2009) 'A technique for dynamic battery model identification in automotive applications using linear parameter varying structures', *Control Engineering Practice*, Vol. 17, No. 10, pp.1190–1201.

Ipek, E. et al. (2021) 'A novel method for SOC estimation of Li-ion batteries using a hybrid machinelearning technique', Vol. 29, No. 1, pp.18–31.

Kim, J. and Cho, B-H. (2011) 'State-of-charge estimation and state-of-health prediction of a Li-ion degraded battery based on an EKF combined with a per-unit system', Vol. 60, No. 9, pp.4249–4260.

Kim, P. and Kim, P. (2017) 'Convolutional neural network', *MATLAB Deep Learning: With Machine Learning, Neural Networks and Artificial Intelligence*, pp.121–147.

Li, J., Deng, Z., Che, Y. et al. (2023) 'Degradation pattern recognition and features extrapolation for battery capacity trajectory prediction', *IEEE Transactions on Transportation Electrification*.

Li, P., Zhang, Z., Xiong, Q. et al. (2020) 'State-of-health estimation and remaining useful life prediction for the lithium-ion battery based on a variant long short term memory neural network', *Journal of Power Sources*, Vol. 459, p.228069.

Ouyang, T., Xu, P., Chen, J. et al. (2020) 'Improved parameters identification and state of charge estimation for lithium-ion battery with real-time optimal forgetting factor', *Electrochimica Acta*, Vol. 353, p.136576.

Patil, P., Deokate, S.T., Bhoite, A. et al. (2023) 'GAN-enhanced medical image synthesis: augmenting CXR data for disease diagnosis and improving deep learning performance', *Journal of Electrical Systems*, Vol. 19, No. 3.

Pfister, H.D. (2017) *Discrete-Time Signal Processing* [online] http://pfister.ee.duke.edu/courses/ece485/dtsp.pdf (accessed 2017).

Pop, V., Bergveld, H.J., Regtien, P.P.L. et al. (2007) 'Battery aging and its influence on the electromotive force', *Journal of the Electrochemical Society*, Vol. 154, No. 8, p.A744.

Prusty, S. et al. (2022a) 'A novel transfer learning technique for detecting breast cancer mammograms using VGG16 bottleneck feature', *ECS Transactions*, Vol. 107, No. 1, p.733.

Prusty, S. et al. (2022b) 'Comparative analysis and prediction of coronary heart disease', *Indonesian Journal of Electrical Engineering and Computer Science*, Vol. 27, No. 2, pp.944–953.

Prusty, S., Patnaik, S., Dash, S.K. (2022c) 'SKCV: stratified K-fold cross-validation on ML classifiers for predicting cervical cancer', *Frontiers in Nanotechnology*, Vol. 4, p.972421.

Prusty, S., Patnaik, S., Dash, S.K. et al. (2024a) 'Predicting cervical cancer risk probabilities using advanced H20 AutoML and local interpretable model-agnostic explanation techniques', *PeerJ Computer Science*, Vol. 10, p.e1916.

Prusty, S., Patnaik, S., Dash, S.K. et al. (2024b) 'SEMeL-LR: an improvised modeling approach using a meta-learning algorithm to classify breast cancer', *Engineering Applications of Artificial Intelligence*, Vol. 129, p.107630.

Rahimi-Eichi, H., Ojha, U., Baronti, F. et al. (2013) 'Battery management system: an overview of its application in the smart grid and electric vehicles', *IEEE Industrial Electronics Magazine*, Vol. 7, No. 2, pp.4–16.

Raijmakers, L.H.J., Danilov, D.L., Eichel, R.A. et al. (2019) 'A review on various temperature-indication methods for Li-ion batteries', *Applied Energy*, Vol. 240, pp.918–945.

Serrao, L. et al. (2011) 'Optimal energy management of hybrid electric vehicles including battery aging', *Proceedings of the 2011 American Control Conference*, IEEE, pp.2125–2130.

Smith, K. and Wang, C-Y. (2006) 'Power and thermal characterization of a lithium-ion battery pack for hybrid-electric vehicles', *Journal of Power Sources*, Vol. 160, No. 1, pp.662–673.

Smith, K.A., Rahn, C.D. and Wang, C.Y. (2009) 'Model-based electrochemical estimation and constraint management for pulse operation of lithium ion batteries', *IEEE Transactions on Control Systems Technology*, Vol. 18, No. 3, pp.654–663.

Sun, F., Hu, X., Zou, Y. et al. (2011) 'Adaptive unscented Kalman filtering for state of charge estimation of a lithium-ion battery for electric vehicles', *Energy*, Vol. 36, No. 5, pp.3531–3540.

Szegedy, C. et al. (2015) 'Going deeper with convolutions', *Proceedings of the IEEE Conference on Computer Vision and Pattern Recognition*, pp.1–9.

Waag, W., Fleischer, C. and Sauer, D.U. (2014) 'Critical review of the methods for monitoring of lithium-ion batteries in electric and hybrid vehicles', *Journal of Power Sources*, Vol. 258, pp.321–339.

Wang, C. (2023) 'A method for identifying and evaluating energy meter data based on big data analysis technology', *International Journal of Information and Communication Technology*, Vol. 23, No. 4, pp.424–445.

Xing, Y., Ma, E.W.M., Tsui, K.L. et al. (2013) 'An ensemble model for predicting the remaining useful performance of lithium-ion batteries', *Microelectronics Reliability*, Vol. 53, No. 6, pp.811–820.

Zeng, L., Wu, T., Ye, T. et al. (2021) 'Modeling galvanostatic charge-discharge of nanoporous supercapacitors', *Nature Computational Science*, Vol. 1, No. 11, pp.725–731.

Zhang, F. (2024) 'Research on accurate estimation of energy consumption of new energy vehicles based on improved Kalman filter', *International Journal of Information and Communication Technology*, Vol. 25, No. 2, pp.181–193.

Zhang, J. et al. (2024) 'A health prediction method for new energy vehicle power batteries based on AACNN-LSTM neural network', *International Journal of Information and Communication Technology*, Vol. 24, No. 5, pp.74–94.

Zhao, Y. and Liu, Y. (2025) 'State of health estimation for lithium-ion batteries based on multi-scale frequency feature and time-domain feature fusion method', *Journal of Electrochemical Energy Conversion and Storage*, Vol. 22, No. 2.